INL/RPT-23-73873
Revision 0

Milestone 1.2.13: Preliminary Measurements of Radiolytic Nitric Acid Formation to Support Predictive Model Validation

July 2023

Ryan P. Morco, Jacy K. Conrad, Kastli D. Schaller, and Gregory P. Holmbeck
Center for Radiation Chemistry Research
Idaho National Laboratory

Idaho National Laboratory

INL is a U.S. Department of Energy National Laboratory
operated by Battelle Energy Alliance, LLC

INL/RPT-23-73873
Revision 0

Milestone 1.2.13: Preliminary Measurements of Radiolytic Nitric Acid Formation to Support Predictive Model Validation

Ryan P. Morco, Jacy K. Conrad, Kastli D. Schaller, and Gregory P. Holmbeck
Center for Radiation Chemistry Research
Idaho National Laboratory

July 2023

Idaho National Laboratory
Center for Radiation Chemistry Research
Idaho Falls, Idaho, 83415

http://www.inl.gov

Prepared for the
U.S. Department of Energy
Office of Environmental Management
Under DOE Idaho Operations Office
Contract DE-AC07-05ID14517

Page intentionally left blank

ABSTRACT

Predictive computational models have been developed to support the technical basis for extended dry storage of aluminum-clad spent nuclear fuel (ASNF) in helium-backfilled cannisters. To date, these models have been optimized on a variety of irradiation experiments designed to elucidate the radiation-induced formation of molecular hydrogen gas, a radiolysis product that is potentially problematic for the safe storage of ASNF. However, the yield of nitric acid (HNO_3) has not been determined, despite conservative predictions of its formation (300–4000 ppm) in 1% residual air environments irradiated in contact with ASNF. HNO_3, another problematic radiolysis product, can lead to enhanced corrosion and potentially compromise storage canister integrity. Thus, to support the validation of predictive computer models, we report the measurement and quantification of HNO_3 from the gamma irradiation of aluminum alloy coupons in humid air.

Page intentionally left blank

ACKNOWLEDGMENTS

This work was supported by the U.S. Department of Environmental Management, Office of Technology Development, under contract DE-AC07-05ID14517.

Page intentionally left blank

CONTENTS

FIGURE

Page intentionally left blank

ACRONYMS AND ABBREVIATIONS

AA1100	Aluminum alloy 1100
γ-AlOOH	Boehmite
$Al(OH)_3$	Gibbsite
Al_2O_3	Alumina
ASNF	Aluminum-clad spent nuclear fuel
DOE	Department of Energy
H_2	Molecular hydrogen gas
He	Helium gas
HNO_2	Nitrous acid
HNO_3	Nitric acid
$^{\bullet}OH$	Hydroxyl radical
N_2	Nitrogen gas
$^{\bullet}NO_2$	Nitrogen dioxide radical

Page intentionally left blank

Milestone 1.2.13: Preliminary Measurements of Radiolytic Nitric Acid Formation to Support Predictive Model Validation

1. INTRODUCTION

The U.S. Department of Energy (DOE) is developing methods for enabling the long-term storage of approximately 14 metric tons of aluminum-clad spent nuclear fuel (ASNF). This fuel is found globally in a broad range of geometries and fuel compositions, and is a waste product generated by research reactors.[1,2] A leading strategy is to subject the ASNF to extended dry storage in helium gas (He)-backfilled DOE-designed sealed canisters,[3–6] the goal being to either use this approach for final disposition or enable interim storage while the highly radioactive isotopes in the fuel decay to a lower radioactivity that allows the ASNF to be processed for ultimate disposition.

Predictive computational models were developed to support the technical basis for this storage approach.[1,7–12] To date, these models have been benchmarked using data collected from irradiation experiments designed to explore the radiation-induced generation of molecular hydrogen gas (H_2) from aluminum corrosion layers and associated surface waters.[13,14] H_2 formation is of particular concern due to its potential capacity to promote aluminum alloy embrittlement, storage cannister pressurization, and/or the formation of potentially flammable gaseous mixtures.[15–18] However, other potentially problematic radiolysis products anticipated under specific ASNF dry storage scenarios have received far less attention. For example, under episodic breathing or canister seal failure conditions, stored ASNF would become exposed to humid air environments that, when irradiated, could generate corrosive and oxidizing nitric acid (HNO_3).[19–27] In fact, calculations predict that, in a DOE standard canister with 1% residual air, HNO_3 will be the second most abundant radiolysis product generated after H_2.[11]

Radiolytic formation of HNO_3 in humid air follows two known mechanisms in which nitrogen gas (N_2), which comprises ~78% of the air in Earth's atmosphere, is oxidized by radiation to form the nitrogen dioxide radical ($^{\bullet}NO_2$).[20–27] The $^{\bullet}NO_2$ radical may then produce HNO_3 by reacting with hydroxyl radicals ($^{\bullet}OH$) arising from water vapor radiolysis:[19]

$$^{\bullet}NO_{2(g)} + {}^{\bullet}OH_{(g)} \rightarrow HNO_{3(g)}. \quad (1)$$

HNO_3 readily dissolves in water, including in small layers of condensate on the surfaces of ASNF or elsewhere inside the stainless-steel DOE standard canister. This enables relatively high concentrations of the acid to form, creating localized low pH and nitrate-ion-containing environments known to promote corrosion. For example, even low concentrations of HNO_3 have been shown to corrode stainless steel at a rate of 0.01–0.034 mils per year penetration.[28]

To date, quantification of the radiolytic yield of HNO_3 produced by the irradiation of ASNF in humid air has not been reported, despite the potential impact of HNO_3 on cladding/canister integrity. Furthermore, the current computer model developed as part of this research program conservatively predicts the formation of 500–3000 ppm HNO_3 in the presence of small amounts of residual air, yet no experimental data exist to validate this calculation.[7] Thus, to support the advancement of this program's modeling capabilities, here we report our preliminary findings on the yield of HNO_3 stemming from the gamma irradiation ($\leq$ 18 MGy) of sealed humid air environments under ambient irradiator temperature (~40°C) conditions, both with and without the inclusion of corroded aluminum alloy 1100 (AA1100) coupons.

2. EXPERIMENTAL METHODS

2.1 Materials

AA1100 coupons (2.5 × 0.65 × 0.15 cm, with a single $^1/_8$-in. diameter hole for mounting) were sourced from Metals Samples Company - Alabama Specialty Products, Inc. (Munford, AL, USA). Acetone (HPLC Plus, ≥ 99.9%), ethanol (absolute, ≥ 99.8%), and HNO_3 (≥ 99.999% trace metals basis) were supplied by MilliporeSigma (Burlington, MA, USA). Ultra-pure water (18.2 MΩ·cm) was generated in-house via a Thermo Fisher Scientific (Waltham, MA, USA) Harvey™ DI+ Cartridge System and used for all water applications. Unless otherwise stated, all materials were used as received.

2.2 Sample Preparation

Prior to gamma irradiation, all AA1100 coupons were pre-corroded for 29 days at 95 ± 1°C, then air-dried, as previously reported.[13,14] Humid air samples were then prepared (both with and without a corroded AA1100 coupon) to evaluate the impact of an interface on the radiation-induced generation of HNO_3. The samples were comprised of flame-sealed, bespoke, borosilicate ampoules containing ambient air equilibrated with 750 µL of water, which was added to a smaller compartment connected to the main body via a narrow neck, as shown in **Figure 1**. This design ensured 100% relative humidity in the system and facilitated the dissolution of radiolytically formed HNO_3 from the gas phase into the water compartment for ease of sampling, all while avoiding direct contact between the added water and the corroded AA1100 coupon.

Figure 1. Bespoke ampoule design.

2.3 Steady-State Gamma Irradiation

The Idaho National Laboratory Center for Radiation Chemistry Research's Foss Therapy Services (North Hollywood, CA, USA) Model 812 cobalt-60 gamma irradiator was used to perform all the irradiations. Samples were loaded in triplicate into a multi-position sample holder and irradiated at ambient irradiator temperature (~40°C, as determined using a calibrated NI USB-TC01 Single Channel Temperature Input Device equipped with a K-type thermocouple) over several weeks. Chemical dosimetry was employed to determine the dose rate at each occupied sample position in the gamma irradiator.[29] The measured dose rates (30–383 Gy min^{-1}) were then corrected for the natural decay of the cobalt-60 sources ($\tau_{1/2}$ = 5.27 years) over the duration of the irradiations. The presented absorbed gamma doses are relative to water.

2.4 Ion Chromatography

Post-irradiation, the sample ampoules were cracked open to measure the amount of HNO_3 in the aqueous phase. The Henry's law constant (k_H) for HNO_3 is very high ($k_H = 2.1 \times 10^5$ mol L^{-1} bar^{-1} at 25°C),[30] meaning that for millimolar (mM) amounts of HNO_3 detected in the aqueous phase, only ~10^{-10} M HNO_3 would remain in the headspace. For this reason, the HNO_3 detected in the aqueous phase by this work was considered to be the total amount of HNO_3 generated in the investigated systems.

Ion chromatography, using a Thermo Fisher Scientific Dionex ICS-5000+ ion chromatograph with a conductivity detector equipped with an eluent conductivity suppressor, was employed to quantify the amount of HNO_3 formed. The column was a Dionex IonPacTM AS11-HC analytical column with an AG-11-HC guard column. The column/compartment temperature was 25°C and the pump flow rate was 0.38 ml min^{-1}. The eluent used in this study was an aqueous solution of potassium hydroxide (KOH) made

from an EGC 500 KOH eluent generator cartridge and degassed deionized water. The eluent was set to an initial concentration of 1 mM KOH for 6 minutes, then increased gradually to 15 mM over 8 minutes, and finally ramped at a faster rate to 30 mM over 6 minutes. Lastly, the KOH was then again increased to 72 mM to flush the column and then decreased back to 1 mM where it was held for 5 minutes to equilibrate the column for the next run—for a total run time of 27 minutes per injection. Calibration curves for nine standard solutions of 0.5–100.0 mM HNO_3 were freshly prepared and injected in triplicate before each set of ion chromatography measurements. All sample injections were repeated in duplicate, and the results were averaged. This method was accurate within ± 8%, as determined against a quality control standard periodically (every 10) injected throughout the run.

3. RESULTS AND DISCUSSION

Figure 2 shows the concentrations of HNO_3 measured by this work for irradiated humid air in both the absence and presence of a corroded AA1100 coupon. In both cases, the irradiated humid air led to the formation of significant amounts of HNO_3; however, in the presence of a corroded AA1100 coupon, this yield was drastically lower. For example, at ~17 MGy, the yield of HNO_3 was 65% lower in the presence of a corroded AA1100 coupon. This observed difference may be attributed to several mechanisms, including (*i*) adsorption of radiolytically formed HNO_3 onto the coupon's heterogenous corrosion layers;[13,14] (*ii*) loss of HNO_3 precursors (i.e., $NO_2^{\bullet}$ and $^{\bullet}OH$) to surface-enhanced processes, thereby inhibiting **Eq. 1**; and/or (*iii*) the reaction of HNO_3 with the various mineral phases comprising the coupon's corrosion layer (e.g., boehmite [γ-AlOOH] and gibbsite [$Al(OH)_3$]).[31,32] The literature gives evidence for the formation of water-solvated nitrate ions on the surface of boehmite and gibbsite powders,[33] potentially supporting the first of the three aforementioned mechanisms; however, more work must be done to determine the exact process or processes at play in this case. Note that, although HNO_3 has been shown to readily react with bare aluminum metal to yield aluminum oxide/alumina (Al_2O_3), there is negligible reaction between HNO_3 and the Al_2O_3 product.

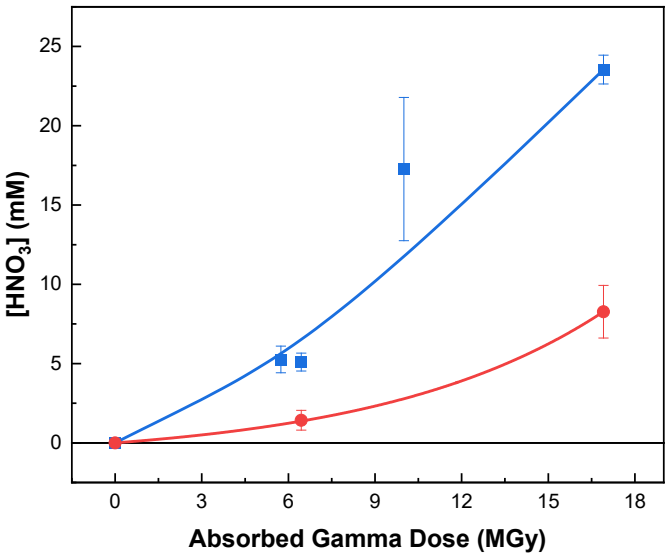

Figure 2. Concentration of HNO_3 measured as a function of absorbed gamma dose from the irradiation of humid air in the absence (■) and presence (●) of a corroded AA1100 coupon. Solid curves are intended for visualization purposes only.

In both irradiated systems, the yield of HNO_3 increases with absorbed gamma dose, exhibiting what appears to be exponential growth behavior. However, additional experiments conducted at higher absorbed doses are needed to confirm this trend. Irrespective of the mechanism, a steady-state yield of HNO_3 was not attained under the investigated conditions, indicating that larger yields are attainable from this system. When compared with the aforementioned conservative model predictions (i.e., a plateau at 500–3000 ppm [7.9–47.6 mM] HNO_3),[7] our measured yields are of a similar order of magnitude. However, current 50-year model calculations at ~0.3 Gy min^{-1} predict that the yield of HNO_3 reaches steady-state within ~8 MGy,[7] which is clearly not the case in our system, given the radiolytic behavior of HNO_3 (see **Figure 2**). The model predictions are not directly comparable to this experimental set, as the model used 1% air, with 1% water vapor in He, as compared to our experiments in 100% humid air. The presence of the He backfill gas as the major gaseous species is expected to substantially reduce the HNO_3 yield because the precursors to its formation will deplete more rapidly at an air and water concentration of only 1%. Furthermore, the extensive literature on HNO_3 radiolysis in aqueous solutions suggests its subsequent degradation to form additional products (e.g., nitrous acid [HNO_2]) that must also be considered in these systems.[34,35] Finally, it has been shown that excited He atoms in the gas phase can ionize N_2 gas via Penning ionization, potentially opening additional pathways for HNO_3 formation.[36] This, together with our new experimental data, suggests room for mechanistic improvement in our current modeling formulism, and further investigation into these phenomena is required.

4. CONCLUSIONS

Overall, the presented preliminary data clearly demonstrate that significant amounts of HNO_3 can form from the gamma irradiation of humid air in the presence of surrogate ASNF coupons. Within the dose range employed here ($\leq$ 18 MGy), a steady-state yield of HNO_3 was not attained; instead, the HNO_3 concentration continued to increase with absorbed gamma dose, contrary to preliminary calculations extending out to ~8 MGy.[7] Although the experimental conditions employed here are not directly comparable to model predictions, our findings highlight several mechanistic discrepancies that require further investigation to improve our current predictive modeling capabilities:

- How much of the HNO_3 formed adsorbs to the surface of the ASNF/canister materials, and how does this impact their integrity?
- Does Penning ionization, as mediated by He excitation, promote or inhibit HNO_3 formation and accumulation?
- Do the radiolysis products of HNO_3 accumulate on surfaces, and how do they interact with the ASNF corrosion layers and canister materials?

5. REFERENCES

[1] E. Eidelpes, et al. (2023). "Technical basis for extended dry storage of aluminum-clad spent nuclear fuel." *J. Nucl. Mat.*, 577 (2023): 154299.

[2] Spent Fuel Database (SFD). 8.0.7 ed.; The Department of Energy, Ed. 2021.

[3] U.S. DOE. (1998). "Preliminary Design Specification for Department of Energy Standardized Spent Nuclear Fuel Canisters Volume 1: Design Specification." (DOE/SNF/REP--011-Vol. 1). United States Department of Energy, Office of Spent Fuel Management and Special Projects. https://www.osti.gov/servlets/purl/665971.

[4] U.S. DOE. (1998). "Preliminary Design, Specification for Department of Energy Standardized Spent Nuclear Fuel Canisters Volume 2." Rationale Document (DOE/SNF/REP--011-Vol. 2) United States Department of Energy, Office of Spent Fuel Management and Special Projects

Idaho. https://inis.iaea.org/search/search.aspx?orig_q=reportnumber:%22DOE/SNF/REP--011-VOL.2%22.

[5] M. D. Argyle. (2017). "Aluminum Clad Spent Nuclear Fuel: Technical Considerations and Challenges for Extended (>50 Years) Dry Storage" 2017.

[6] M. J. Connolly. (2017). "Aluminum Clad Spent Nuclear Fuel Long Term Dry Storage Technical Issues Action Plan – Technical and Engineering Activities."

[7] A. W. Abboud. (2021). "Modeling Summary of ASNF in DOE Sealed Standard Canisters." INL/EXT-21-64413 2021, Rev. 0, Idaho National Laboratory, Idaho Falls, ID. https://doi.org/10.2172/1924435.

[8] A. W. Abboud. (2021). "Modeling of Radiolytic Hydrogen Generation of Irradiated Surrogate Aluminum Plates." INL-RPT-21-66504, Rev. 0, Idaho National Laboratory, Idaho Falls, ID. https://doi.org/10.2172/1924440.

[9] A. W. Abboud. (2022). "Extended Modeling of DOE Sealed Canisters with Updated Chemistry Models." INL-RPT-22-67694, Rev. 0, Idaho National Laboratory, Idaho Falls, ID. https://doi.org/10.2172/1924453.

[10] A. W. Abboud. (2022). "Sensitivity study of coupled chemical-CFD simulations for analyzing aluminum-clad spent nuclear fuel storage in sealed canisters." *Nucl. Eng. Des.*, 390 (2022): 111691. https://doi.org/10.1016/j.nucengdes.2022.111691.

[11] A. W. Abboud and R. Morco. (2023). "Chemical Model of Pressure Bounding Conditions in a DOE Standard Canister." INL/RPT-23-70934, Idaho National Laboratory, Idaho Falls, ID.

[12] A. W. Abboud. (2023). "Modeling DOE Standard Canister Configurations with Updated Surface Chemistry." INL/RPT-23-73230, Idaho National Laboratory, Idaho Falls, ID.

[13] E. H. Parker-Quaife, C. Verst, C. R. Heathman, P. Z. Zalupski, and G. P. Horne. (2020). "Radiation-Induced Molecular Hydrogen Gas Generation in the Presence of Aluminum Alloy 1100." *Rad. Phys. Chem.*, 177 (2020): 109117. https://doi.org/10.1016/j.radphyschem.2020.109117.

[14] J. K. Conrad. (2022). "Radiolytic Gas Production from Aluminum Coupons (Alloy 1100 and 6061) in Helium Environments – Assessing the Extended Storage of Aluminum Clad Spent Nuclear Fuel." *MDPI Mat.,* 15, no. 20 (2022): p. 7317. https://doi.org/10.3390/ma15207317.

[15] R. Ambat and E. S. Dwarakadasa. (1996). "Effect of hydrogen in aluminum and aluminum alloys: A review." *Bull. Mater. Sci.,* 19 (1996): pp. 103–114. https://doi.org/10.1007/BF02744792.

[16] R. P. Gangloff and B. P. Somerday. (2012). *Gaseous Hydrogen Embrittlement of Materials in Energy Technologies* – Volume 1: The problem, its characterization and effects on particular alloy classes." ISBN: 9781845696771, *Elsevier Science/Woodhead Publishing Limited*, Philadelphia, PA. https://shop.elsevier.com/books/gaseous-hydrogen-embrittlement-of-materials-in-energy-technologies/gangloff/978-1-84569-677-1.

[17] G. Lu and E. Kaxiras. (2005). "Hydrogen Embrittlement of Aluminum: The Crucial Role of Vacancies." *Phys. Rev. Lett.*, 94 (2005): 155501. https://doi.org/10.1103/PhysRevLett.94.155501.

[18] B. Bonin, M. Colin, and A. Dutfoy. (2000). "Pressure building during the early stages of gas production in a radioactive waste repository." ISSN :0022-3115, *J. Nucl. Mat.,* 281, no. 1 (2000): pp. 1-14. https://www.infona.pl/resource/bwmeta1.element.elsevier-75bb2ca0-8c7c-3296-adaf-166b247b4067.

[19] R. P. Morco, J. M. Joseph, D .S. Hall, C. Medri, D. W. Shoesmith, and J. C. Wren. (2017). "Modelling of radiolytic production of HNO_3 relevant to corrosion of a used fuel container in deep geologic repository environments." *Corros. Eng. Sci. Techn.*, 52, no. 1 (2017): pp. 141–147. https://doi.org/10.1080/1478422X.2017.1340227.

[20] M. T. Dmitriev. (1958). "The Radiation Oxidation of Nitrogen .3. Some Questions Concerning the Mechanism of the Reaction and a Comparison with Electrical Discharge Data." *Zh Fiz Khim+*, 32, no. 10 (1958): p. 2418.

[21] M. T. Dmitriev and S. Y. Pshezhetskii. (1959). "The Radiation Oxidation of Nitrogen .4. Temperature Dependence and the Role of Ions in the Reaction under the Action of Fast Electrons. *Zh Fiz Khim+,* 33, no. 2 (1959): p. 463.

[22] M. T. Dmitriev and S. Y. Pshezhetskii. (1960). "Radiation Oxidation of Nitrogen .5. The Kinetics of Nitrogen Oxidation Induced by Gamma-Radiation and the Part Played by Ion Recombination." *Zh Fiz Khim+*, 34, no. 4 (1960): p. 880.

[23] P. Harteck and S. Dondes. (1956). "Fixation of Nitrogen by Ionizing Radiation as Nitrogen Dioxide and Nitrous Oxide." *J. Chem. Phys.,* 24, no. 3 (1956): p. 619. https://doi.org/10.1063/1.1742561.

[24] P. Harteck and S. Dondes. (1957). "Decomposition of Nitric Oxide and Nitrogen Dioxide by the Impact of Fission Fragments of Uranium-235." *J. Chem. Phys*., 27, no. 2 (1957): pp. 546–551. https://doi.org/10.1063/1.1743766.

[25] P. Harteck and S. Dondes. (1958). "Nitrogen Pentoxide Formation by Ionizing Radiation. *J. Chem. Phys.,* 28, no. 5 (1958): pp. 975–976. https://doi.org/10.1063/1.1744307.

[26] P. Harteck and S. Dondes. (1959). "The Kinetic Radiation Equilibrium of Air." *J. Phys. Chem.,* 63, no. 6 (1959): pp. 956–961. https://doi.org/10.1021/j150576a043

[27] P. Harteck and S. Dondes, Radiation Chemistry of Fixation of Nitrogen. *Science*, 146, no. 364 (1964): pp. 30–35. https://doi.org/10.1126/science.146.3640.30.

[28] G. G. Kolman, D. K. Ford, D. P. Butt, and T. O. Nelson. (1997). "Corrosion of 304 stainless steel exposed to nitric acid-chloride environments." *Corrosion Science,* 39, no. 12 (1997): pp. 2067–2093. https://doi.org/10.1016/S0010-938X(97)00092-9.

[29] H. Fricke and E. J. Hart. (1935). "The Oxidation of Fe^{2+} to Fe^{3+} by the Irradiation with *X*-Rays of Solutions of Ferrous Sulfate in Sulfuric Acid." *J. Chem. Phys.,* 3 (1935): p. 60.

[30] R. Sander. (2015). "Compilation of Henry's law constants (version 4.0) for water as solvent." *Atmos. Chem. Phys.* 15, no. 8 (2015): pp. 4399–4981. https://doi.org/10.5194/acp-15-4399-2015.

[31] P. R. Bloom. (1983). "The Kinetics of Gibbsite Dissolution in Nitric Acid." *Soil Science Society of America Journal*, 47, no. 1 (1983): pp. 164–168. https://doi.org/10.2136/sssaj1983.03615995004700010032x.

[32] C. D. Peskleway, G. S. Henderson, and F. J. Wicks. (2003). "Dissolution of gibbsite: Direct observations using fluid cell atomic force microscopy." *American Mineralogist*, 88, no.1 (2003): pp. 18–26. https://pubs.geoscienceworld.org/msa/ammin/article-abstract/88/1/18/43776/Dissolution-of-gibbsite-Direct-observations-using?redirectedFrom=fulltext. https://doi.org/10.2138/am-2003-0103.

[33] M. W. Ross and T. C. DeVore. (2008). "Desorption of Nitric Acid from Boehmite and Gibbsite." *J. Phys. Chem. A,* 112, no. 29 (2008): pp. 6609–6620. https://doi.org/10.1021/jp7110555.

[34] G. P. Horne, T. A. Donoclift, H. E. Sims, R. M. Orr, and S. M. Pimblott.(2016). "Multi-scale modeling of the gamma radiolysis of nitrate solutions." *J. Phys. Chem. B,* 120, no. 45 (2016): 11781–11789. https://doi.org/10.1021/acs.jpcb.6b06862.

[35] G. P. Horne, S. M. Pimblott, and J. A. LaVerne. (2017). "Inhibition of Radiolytic Molecular Hydrogen Formation by Quenching of Excited State Water." *J. Phys. Chem. B,* 121, no. 21 (2017): 5385–5390. https://doi.org/10.1021/acs.jpcb.7b02775.

[36] D. C. Dunlavy and P. E. Siska. (1996). "Probing the Transition State of the He*(2 U^1S) + N_2 Penning Ionization Reaction with Electron Spectroscopy." *J. Phys. Chem.*, 100, no. 1 (1996): 21–29. https://doi.org/10.1021/jp952230j.